

Analytical Modelling Approach for Switched Reluctance Machines with Deep Saturation

Xiaofeng Ding, Mohamed Rashed, Christopher Ian Hill, Serhiy Bozhko

Department of Electrical and Electronic Engineering

University of Nottingham, UK

eexxd8@nottingham.ac.uk

Abstract—This paper presents an analytical modelling approach for Switched Reluctance Machines (SRMs) with a wide saturation range. There are many existing analytical modelling approaches in literature that give good accuracy, however most do not consider modelling accuracy in the deeply saturated region of operation. The proposed modelling method is suitable for SRMs operating under the entire saturation range. The proposed methodology begins by modelling the inductance profile as a Fourier series in order to take advantage of its approximately sinusoidal variation with respect to rotor position. Improvements are then presented to achieve higher accuracy. Flux linkage and torque models for the SRM can then be derived from the inductance model. An example 60kW 6/4 SRM with a wide saturation operating range is used for analytical modelling. It is shown that high accuracy is obtained by the derived analytical model when evaluated against the measured magnetic characteristics of the machine.

Keywords—switched reluctance machine (SRM), more electric aircraft (MEA), analytical model, inductance profile.

I. INTRODUCTION

In modern more electric aircraft (MEA), reduction of overall weight is a major research topic [1]. The starter/generator (S/G) concept is commonly accepted as a next generation solution to reduce overall on-board weight [2]. The S/G utilizes a single machine which operates in both motoring and generation modes on demand. A commonly studied candidate for the S/G is the permanent magnet synchronous machine (PMSM), mainly because of its high power density and well established control scheme. However, another popular candidate is the switched reluctance machine (SRM). The SRM has distinct advantages over the PMSM in terms of robustness, high temperature operation, low inertia and low cost manufacture [3, 4]. This paper therefore focuses on SRMs as a potential alternative solution for S/G systems.

Accurate modelling of SRMs is essential in order to achieve high performance control of aircraft S/Gs. The model is used in many places within the control algorithms of the SRM, e.g. to determine the reference current waveform for each phase based on the measured rotor position. However, the SRM is often operated under magnetic saturation and as such the machine model is highly nonlinear. This therefore makes derivation and implementation of accurate models a difficult task. Look-up tables can be utilized but they are complex to use, require large computational memory and result in a piecewise type of model which limits the flexibility and accuracy. Alternatively, analytically derived models can be directly

implemented into the control algorithms. The use of these models is much more flexible as they are much easier to manipulate and transform to different forms for control design and implementation purposes.

In this paper it will be shown how an accurate analytical model of a SRM, operated deeply saturated region, can be derived from measured magnetic characteristics. The majority of the analytical modelling approaches presented in literature can provide accurate modelling for SRMs operating under shallow saturation. However, for SRMs which are normally characterized by operation under deep saturation, it is difficult to obtain an analytical model that can provide accurate modelling for the entire operating range and level of saturation, i.e. for both linear and deep saturation regions of SRM operation. For example, an efficient flux linkage-based model of a SRM has been proposed in [5], this modelling technique requires a minimum of only five data points which should be obtained through finite element analysis (FEA). The flux linkage is derived from inductance profile which is expressed as a Fourier series. The coefficients of the inductance expression are based on nonlinear generic model. This method can provide good accuracy when the SRM is in linear or shallow saturated region. While the SRM operates in deeply saturated region, the generic model-based method would not be able to provide high accuracy. In [6], the author presented direct flux linkage modelling of a SRM which only operated within a relatively shallow saturation region. This work did however provide an innovative solution for modelling flux linkage with a limited amount of measured data. Unfortunately, when operating under deep saturation, the accuracy of this method drops significantly. The method in [7] provides an analytical circuit model which has high accuracy. This model treats flux linkage as multiple decoupled one-argument functions (i.e. either current or rotor position). However, the method is more complex to apply. In [8], the modelling approach presented considers operation of the SRM within the saturated regions. This method gives a good result even in the deeply saturated region, however it requires SRM geometric and electrical parameters for FEA to compute flux linkage and torque characteristics.

This paper will detail the development of an easy-to-use analytical model for high power density SRMs that maintains accuracy over the entire range of operation, including the deeply saturated region. The proposed modelling technique is based on inductance profiles derived from measured flux linkage data points.

II. SWITCHED RELUCTANCE MACHINE CONFIGURATION

For typical configurations of SRMs, the stator/rotor pole count is usually chosen to be even numbered in order to form a balanced multiple phase system. The number of rotor and stator poles are normally reasonably close, as this will increase the potential average value of torque produced [9]. The popular configurations of SRMs are 3-phase and 4-phase with 6/4 and 8/6 stator/rotor poles. Increasing of the number of phases will in general decrease the torque ripple of the SRM; however, it will also increase the difficulty of manufacture and hence the cost. It should be noted that if the number of phases is lower than 3, the SRM has no ability to self-start.

Overall, the selection of stator/rotor pole numbers is a balance between torque ripple, self-starting and minimization of iron losses. Therefore, this has to be selected appropriately for the given application. In our study, a 6/4 configuration is selected for high speed aircraft S/G application because it offers the best compromise in terms of safety, reliability and cost [10]. Figure 1 shows the simplified structure of a 6/4 SRM.

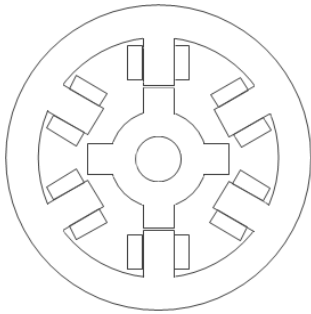


Fig. 1. Typical 6/4 Switched Reluctance Motor

III. ANALYTICAL MODELLING OF THE SWITCHED RELUCTANCE MACHINE

In this section, the development of an analytical model for SRMs will be presented, together with specific analysis of a well-documented 60kW 6/4 SRM with deep saturation [11]. Most of the analytical modelling approaches available for SRMs tend to start with modelling of flux-linkage profiles (e.g. [6, 12]) from which the inductance and torque profiles are obtained. Instead, in this paper, the proposed modelling approach will start with the inductance profile in order to take advantage of its near sinusoidal variation against rotor position.

A. Flux Linkage, Inductance and Torque Profiles

The magnetization characteristics, i.e. flux linkage profile $\Psi(i, \theta)$, give all the information needed to build the model of the SRM. The flux linkage profile can be acquired either from FEA of the machine or by experimental measurements [13]. The more data acquired, the more accurate and closer the obtained model will be to the actual machine characteristics. Figure 2 shows the flux linkage profile of the machine studied in this paper, the flux linkage data points were measured with the rotor position from $0 - 45^\circ$ with a resolution of 5° and the excitation current from $0 - 450\text{A}$ with a resolution of 45A . It should be noted that over the full operational current range, the flux-linkage/current profile shows different behaviors according to level of excitation current. The full current range can be divided into 3 regions:

Region I - linear region, Region II – shallow saturation region and Region III – deep saturation region. There are no exact thresholds of these regions. However, these thresholds can be defined based on the design specification of the machine, e.g. the deep saturation region can be enlarged and hence represent a significant portion of the flux profile if the machine is to be characterized for high torque density design.

The inductance profile is calculated from the flux profile by the following relationship:

$$L(i, \theta) = \Psi(i, \theta) / i \quad (1)$$

where L is the inductance, i is the excitation current, θ is the rotor position.

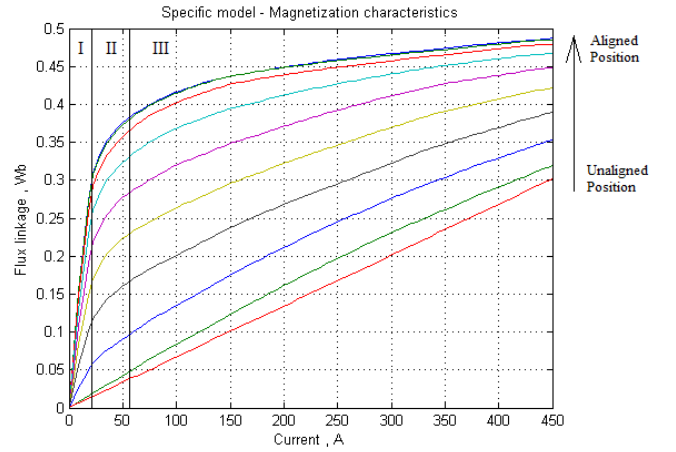


Fig. 2. Magnetization characteristics of SRM

The torque profile is derived from the concept of co-energy which is expressed as:

$$T(i, \theta) = \partial W'(i, \theta) / \partial \theta |_{i=I_c} = \partial \left(\int_0^i \Psi(i, \theta) di \right) / \partial \theta |_{i=I_c} \quad (2)$$

where W' is co-energy and I_c is the excitation current. The torque calculations are repeated for different values of I_c in order to obtain the torque profile for the entire current excitation range.

B. Proposed Analytical Modelling Approach

The inductance profile for the SRM studied in this research was obtained and is presented in Figure 3. The figure clearly shows the significant variation of inductance in respect of current and rotor position. The values in Figure 3 are derived from the magnetization characteristics shown in Figure 2.

The inductance profile is periodic against rotor position. A full period of this waveform is shown in Figure 3. The stator and rotor are aligned when $\theta = 0^\circ$ or $\theta = 90^\circ$, the unaligned position is when $\theta = 45^\circ$. It is symmetrical along $\theta = 0^\circ$ and $\theta = 45^\circ$. This indicates that the SRM is a 6/4 structure. It can also be seen from Figure 3 that the inductance profile variation is approximately sinusoidal for each excitation current. Because of the periodic nature of the inductance profile, it can be represented by an analytical model based on a 2-term Fourier series, as given (3).

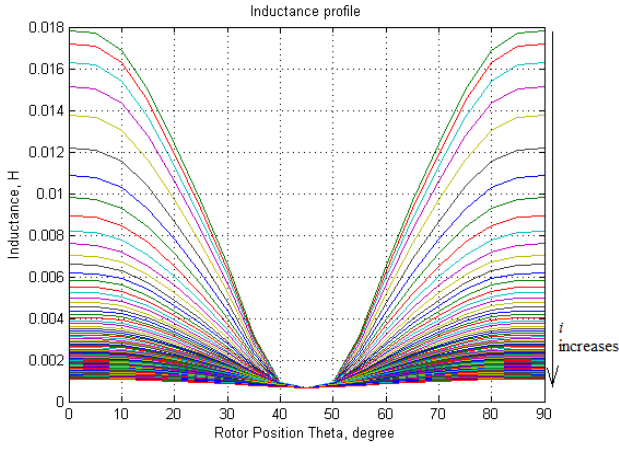


Fig. 3. Studied SRM inductance profile

$$L(i, \theta) = a_0(i) + a_1(i) \cos(\omega_1 \theta) + a_2(i) \cos(2\omega_1 \theta) \quad (3)$$

where the coefficients a_0 , a_1 and a_2 are constant values for any given current value and are solely related to excitation current. The Fundamental frequency, ω_1 , in (3) is defined as $\omega_1 = \pi/(\theta_{max} - \theta_{min})$. θ_{max} and θ_{min} are the rotor angles of the unaligned position and the aligned position respectively.

By applying (3) to the corresponding inductance profile from Figure 3 the coefficients a_0 , a_1 and a_2 can be obtained for each excitation current, i . After obtaining a_0 , a_1 and a_2 for the entire excitation current range, there will be three sets of data which represent the variation of the Fourier series coefficients against the excitation current. These are given by $a_0(i)$, $a_1(i)$ and $a_2(i)$. Each of these coefficients can be represented as a combined exponential function with respect to the excitation current:

$$a_n(i) = A_n e^{B_n i} + C_n e^{D_n i}, n = 0,1,2 \quad (4)$$

By performing curve fitting in Matlab for $a_0(i)$, $a_1(i)$ and $a_2(i)$, three sets of related coefficients (A_1, B_1, C_1 and D_1) are obtained. Once obtained, these coefficients complete the analytical model of the inductance profiles given by (3).

The inductance profile in Figure 3 for the 60kW 6/4 SRM studied in this paper was modelled using (3), (4). The coefficients of the analytical model were obtained and are given in table I.

TABLE I. COEFFICIENTS OBTAINED BY CURVE FITTING

n	A_n	B_n	C_n	D_n
0	9.32e-03	-2.61e-02	2.48e-03	-2.29e-03
1	8.21e-03	-2.83e-02	2.18e-03	-5.61e-03
2	-8.88e-04	-2.05e-02	-2.26e-04	-3.51e-03

According to the obtained analytical model, the inductance, and flux linkage profiles are calculated and presented in Figures 4 and 5.

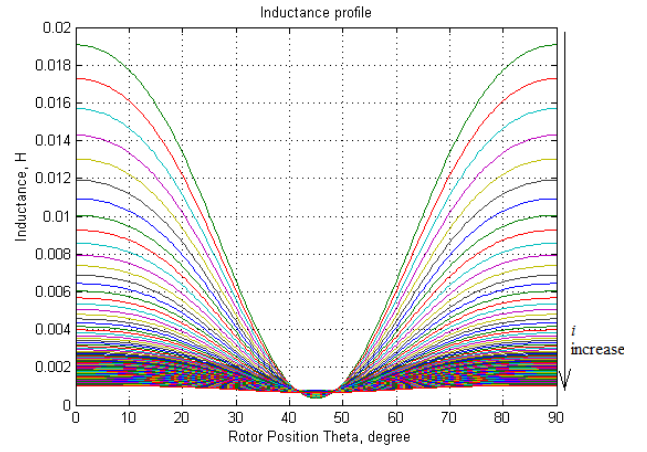


Fig. 4. Calculated inductance profile

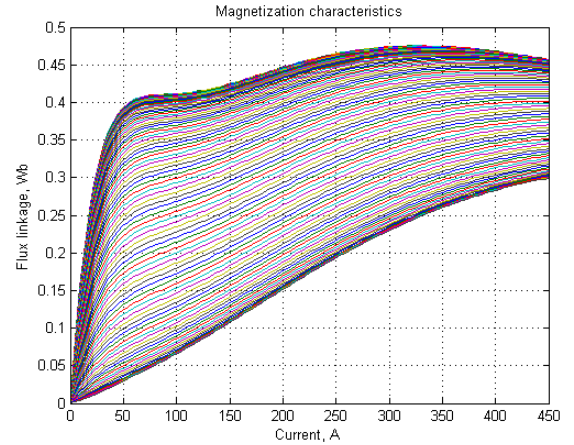


Fig. 5. Calculated flux linkage profile

It should be noted from Figures 4 and 5 that the inductance and flux profiles obtained from the derived analytical model (3) do not match the actual data shown in Figures 3 and 2, e.g. the inductance profiles at the unaligned position in Figure 4 does not converge to the expected value of unaligned inductance. Moreover, the gradients of the flux linkage profiles in the deep saturation region are not constant as expected, but it has a kind of superimposed sinusoidal variation.

To overcome this problem, the inductance profile model in (3) is modified to guarantee that all the inductance profiles for different excitation currents converge to the same value of unaligned inductance. The modified model is detailed in the following section.

C. Modified Inductance Profile Model

The pre-adjusted inductance analytical model (3) always results in distortion compared to the original waveform. Further modification is required in order to minimise the distortion.

The model (3) is re-formulated to guarantee that for all inductance profiles the value of the inductance is equal at the unaligned position. This is achieved by omitting the DC component of the Fourier series for each inductance profile and then shifting all AC components vertically by re-assigning the minima of their variation to be equal to zero. The shifted AC

components are combined with a DC component which is obtained from the original inductance profile at the unaligned position and derived from the original magnetization characteristics. The modified analytical model can therefore be expressed as:

$$L(i, \theta) = L_0 + a_1(i) (1 + \cos(\omega_1\theta)) + a_2(i) (-1 + \cos(2\omega_1\theta)) \quad (5)$$

where L_0 is the original inductance at the unaligned position, $a_1(i)$ and $a_2(i)$ are given by (4).

For the SRM studied in this research, the original inductance at the unaligned position was acquired from Figure 3. In this case L_0 was found to be 0.00067 H. The shifted AC components (fundamental and second order) of the studied SRM, given in (5), are shown in Figures 6 and 7.

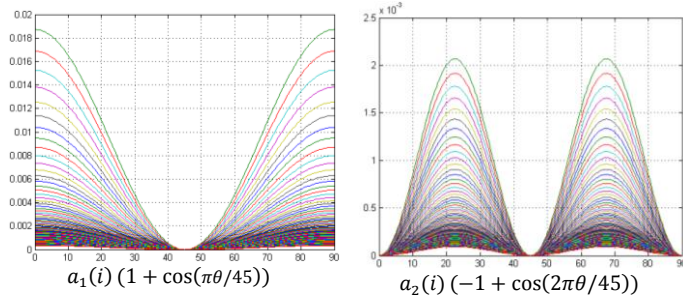


Fig. 6. Shifted fundamental component

Fig. 7. Shifted 2nd harmonic component

The figures indicate that the fundamental and 2nd harmonic components are shifted from original positions to match the same minimal values; these are then set to be zero. The AC components are further shifted vertically by a value equal to L_0 . The inductance, flux linkage and torque profiles for the studied SRM were calculated based on the model given by (5) and are presented in Figures 8-10.

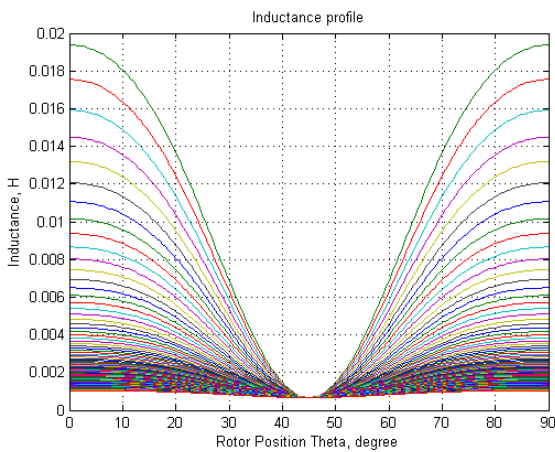


Fig. 8. Inductance profile with 1st improvement

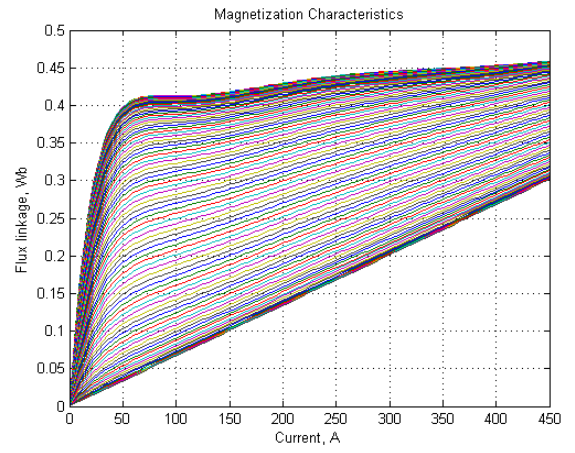


Fig. 9. Flux linkage profile with 1st improvement

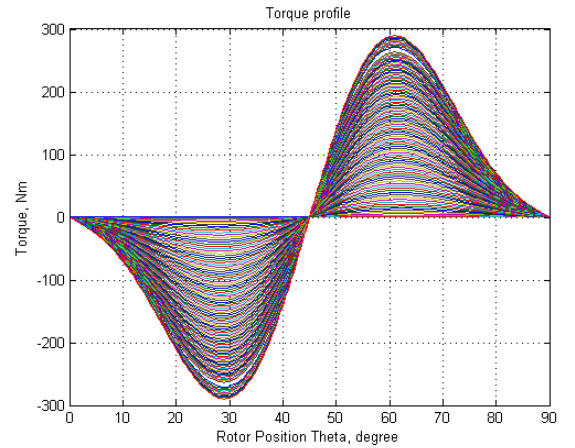


Fig. 10. Torque profile with 1st improvement

The modified analytical model (5) significantly reduces the major distortion on the waveform of each profile in comparison to the profiles shown previously in Figures 4 and 5 for the original model (3). However, the modelling accuracy can still be further improved. The second step of improvement, which aims to further reduce the error/distortion in the deep saturation region, is introduced by adding two adjustable weighting factors (X and Y) into the Fourier series coefficient equations (4). The new unified equations for the coefficients within (5) are shown in (6). Therefore (6) now replaces (4).

$$a_n(i) = X A_n e^{B_n i} + Y C_n e^{D_n i}, n = 1, 2 \quad (6)$$

First, the weighting factors X and Y are set equal to 1 and a curve fitting algorithm is applied to obtain the coefficients of (6) i.e. A_n , B_n , C_n and D_n . Subsequently, X and Y are adjusted by trial and error based on the experience gained. The aim is to minimise the remaining distortion in the flux linkage profile in the deep saturation region (see Figure 12). By adjusting X and Y , rebuilding the waveform for each profile and comparing with earlier results to minimise error the optimal selection of constants (X_0 , Y_0) can be found. Once found, the analytical modelling of the inductance is complete.

D. Derivation of Flux Linkage and Torque Analytical Models

From a control point of view, the analytical models of flux linkage and torque are as important as the inductance model, as they are more often used as control variables /references.

The flux linkage analytical model can be easily derived by combining equation (1) and (5):

$$\Psi(i, \theta) = L_0 i + a_1(i) (1 + \cos(\omega_1 \theta)) i + a_2(i) (-1 + \cos(2\omega_1 \theta)) i \quad (7)$$

where the $a_n(i)$ is defined in (6).

The torque analytical model is derived from expressions (2), (5) and (6). This is a more complicated process. The torque analytical model is given by:

$$T(i, \theta) = -180/\pi (K_1(i)\omega_1 \sin(\omega_1 \theta) + 2K_2(i)\omega_1 \sin(2\omega_1 \theta)) \quad (8)$$

where

$$K_n(i) = X_0 A_n (B_n i - 1) e^{B_n i / B_n^2} + Y_0 C_n (D_n i - 1) e^{D_n i / D_n^2} + X_0 A_n / B_n^2 + Y_0 C_n / D_n^2; \quad n = 1, 2 \quad (9)$$

For the SRM studied in this research, the factors are chosen as: $X_0=0.85$ and $Y_0=1.1$. Using equation (5), (6), (7), (8), (9) and the coefficients in Table I, the final analytical model can be derived and used to calculate each profile. The calculated profiles are presented in Figures 11-13.

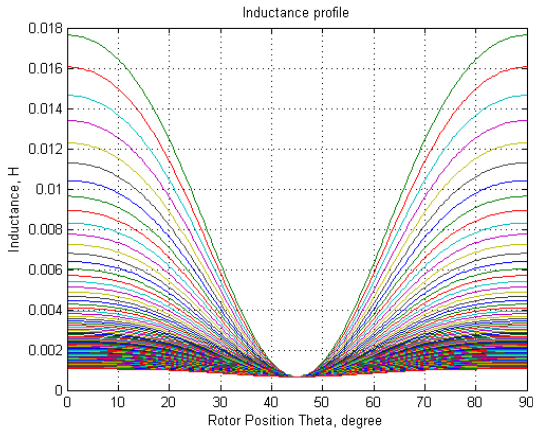


Fig. 11. Final inductance profile

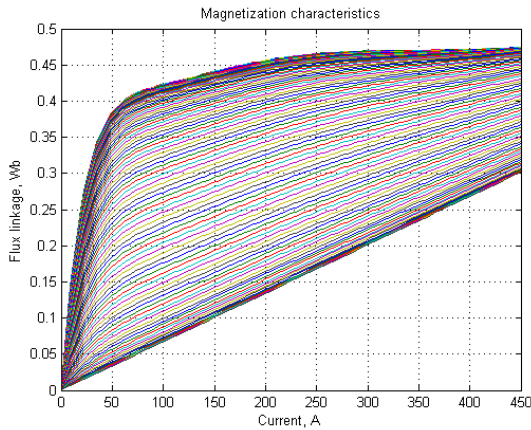


Fig. 12. Final flux linkage profile

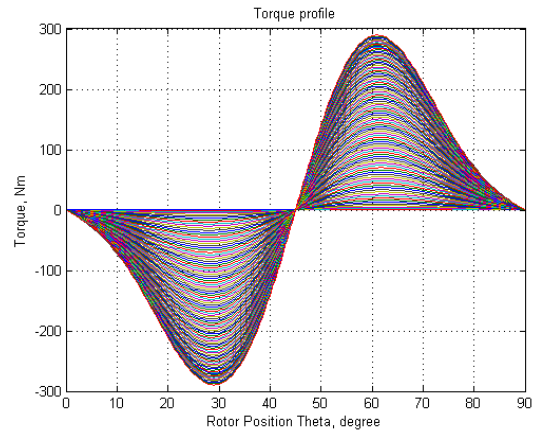


Fig. 13. Final torque profile

The inductance profile in Figure 11 shows a good match to the shape of original profile. It gives minor error in low current situation when the rotor is near the aligned position. When in higher current cases, the modelled inductance profile follows the original profile accurately. The flux linkage profiles in Figure 12 have been improved significantly due to the introduction of weighting factors. The transitional area between linear and nonlinear regions is closer to the actual profile, also the flux linkage is more ‘flat’ and less oscillatory in the deeply saturated region compared to the pre-adjusted flux linkage profile in Figure 5. The torque profiles calculated from the improved model are presented in Figure 13. The waveform has a visually noticeable improvement compared to Figure 10, especially for medium-high current curves where the ‘gap’ has disappeared.

Visual inspection of the analytical profiles shown in Figures 11-13 suggests good, accurate modelling of the 60kW 6/4 SRM studied in this research (i.e. the shape of each modelled profile tracks the original profile closely). In the next section numerical error analysis for inductance and flux linkage profiles will be presented.

E. Error Analysis

In this section the errors of inductance and flux linkage in the pre-adjusted model (3) and (4), the improved model after the first stage (5) and (4) and final model (5) and (6) will be presented and compared in order to verify the improvements made during each stage. In order to compare the results from the analytical model and the original profiles, the range of (i, θ) needs to be addressed. The range of comparison for i is selected to be 0-450A with the step size of 45A, θ is selected to be 0-45° (i.e. variation from the aligned position to the unaligned position) with a step size of 5° in order to match the resolution of original measured data for comparison purposes.

Table II shows the maximum errors between analytical models and the original profiles for each modelling stage. Figures 14-15 show graphical comparisons between the calculated and the actual profiles. Please note that in the table below, for inductance profiles, condition $i = 0A$ means current indefinitely approaches to zero, therefore the value of inductance under this condition is an extreme value.

TABLE II. MAXIMUM ERRORS IN EACH PROFILES FOR EACH MODEL

		Pre-adjusted model	First stage improved model	Final improved model
Inductance (H)	Absolute Error	1.23E-03	1.55E-03	4.51E-04
	Condition (i, θ)	0A, 0°	0A, 0°	0A, 10°
	Relative Error	6.91%	8.67%	2.67%
Flux linkage (Wb)	Absolute Error	3.02E-02	2.82E-02	2.15E-02
	Condition (i, θ)	450A, 0°	450A, 0°	315A, 35°
	Relative Error	15.03%	5.78%	7.57%

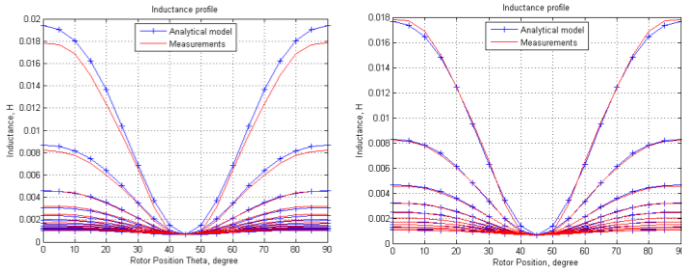


Fig. 14. Compared inductance profile of 1st and final step of improvement

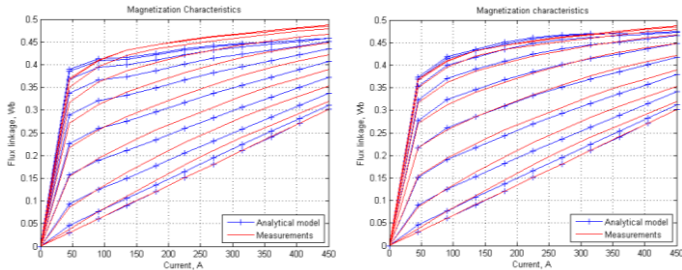


Fig. 15. Compared flux linkage profile of 1st and final step of improvement

The results of inductance and flux linkage show that after improvements, the absolute errors and relative errors have reduced significantly. Comparing the results of the first stage improved model with the final model, the maximum absolute errors in inductance and flux linkage are reduced. It can be seen that the maximum relative error of flux linkage becomes higher, that is because the given current and rotor position conditions are different (i.e. the exact values are different). The final model gives a better overall shape of each profile as well as better tracking performance as shown in Figures 14-15. Overall, the results shown in Table II and shown in Figures 15-16 confirm that this technique produces accurate analytical models for SRMs even when underrating under deep saturation conditions.

IV. CONCLUSIONS

This paper has introduced an analytical modelling method for SRMs. It is based on a Fourier series modeling approach. In

contrast to existing analytical modelling methods, this method starts with inductance profiles in order to take advantage of their sinusoidal nature. This approach is not only suitable for SRMs with shallow saturation but also for those with deep saturation regions such as high power density SRMs. The analytical models for a 60kW, 6/4 SRM have been derived and a comparative error analysis with the measured magnetic characteristics of the SRM has been performed. The results indicate that the proposed modelling method has the ability to describe the machine magnetic characteristics with good accuracy for wide range of excitation current including the deeply saturated operating region.

REFERENCES

- [1] B. Sarlioglu and C. T. Morris, "More Electric Aircraft: Review, Challenges, and Opportunities for Commercial Transport Aircraft," in *IEEE Transactions on Transportation Electrification*, vol. 1, no. 1, pp. 54-64, June 2015.
- [2] A. N. Reshetnikov and A. S. Khlebnikov, "Modeling of integrated starter-generator in generator mode," *2014 15th International Conference of Young Specialists on Micro/Nanotechnologies and Electron Devices (EDM)*, Novosibirsk, 2014, pp. 453-455.
- [3] N. Schofield and S. A. Long, "Generator operation of a switched reluctance starter/generator at extended speeds," *2005 IEEE Vehicle Power and Propulsion Conference*, 2005, pp. 8 pp.-.
- [4] B. Fahimi, A. Emadi and R. B. Sepe, "A switched reluctance machine-based starter/alternator for more electric cars," in *IEEE Transactions on Energy Conversion*, vol. 19, no. 1, pp. 116-124, March 2004.
- [5] H. P. Chi, R. L. Lin and J. F. Chen, "Simplified flux-linkage model for switched-reluctance motors," in *IEE Proceedings - Electric Power Applications*, vol. 152, no. 3, pp. 577-583, 6 May 2005.
- [6] S. Song, M. Zhang and L. Ge, "A New Decoupled Analytical Modeling Method for Switched Reluctance Machine," in *IEEE Transactions on Magnetics*, vol. 51, no. 3, pp. 1-4, March 2015.
- [7] D. Lin, P. Zhou, S. Stanton and Z. J. Cendes, "An Analytical Circuit Model of Switched Reluctance Motors," in *IEEE Transactions on Magnetics*, vol. 45, no. 12, pp. 5368-5375, Dec. 2009.
- [8] H. Hannoun, M. Hilairet and C. Marchand, "Analytical modeling of switched reluctance machines including saturation," *2007 IEEE International Electric Machines & Drives Conference*, Antalya, 2007, pp. 564-568.
- [9] R. Vandana, S. Nikam and B. G. Fernandes, "Criteria for design of high performance switched reluctance motor," *Electrical Machines (ICEM), 2012 XXth International Conference on*, Marseille, 2012, pp. 129-135
- [10] Borg Bartolo, J. and Gerada, C., "Design and Modeling of a 45kW, Switched Reluctance Starter-Generator for a Regional Jet Application," *SAE Technical Paper*, 2014-01-2158, 2014
- [11] D. A. Torrey, X. M. Niu and E. J. Unkauf, "Analytical modelling of variable-reluctance machine magnetisation characteristics," in *IEE Proceedings - Electric Power Applications*, vol. 142, no. 1, pp. 14-22, Jan 1995.
- [12] H. Le-Huy and P. Brunelle, "A versatile nonlinear switched reluctance motor model in Simulink using realistic and analytical magnetization characteristics," *31st Annual Conference of IEEE Industrial Electronics Society, 2005. IECON 2005.*, 2005, pp. 6 pp.-.
- [13] P. Andrada, E. Martinez, J. I. Perat, J. A. Sanchez and M. Torrent, "Experimental determination of magnetic characteristics of electrical machines," *Industry Applications Conference, 2000. Conference Record of the 2000 IEEE*, Rome, 2000, pp. 263-268 vol.1.